Mon. Not. R. Astron. Soc. **000**, 1–9 (2001)

Resolved shocks in clumpy media

R.J.R. Williams[1] and J.E. Dyson[2]
[1] *Department of Physics and Astronomy, Cardiff University, PO Box 913, Cardiff CF24 3YB*
[2] *Department of Physics and Astronomy, University of Leeds, Leeds LS2 9JT*

Received **INSERT**; in original form **INSERT**

ABSTRACT
We study the structure of shocks in clumpy media, using a multifluid formalism. As expected, shocks broaden as they weaken: for sufficiently weak shocks, no viscous subshock appears in the structure. This has significant implications for the survival of dense clouds in regions overrun by shocks in a wide range of astrophysical circumstances, from planetary nebulae to the nuclei of starburst galaxies.

Key words: Hydrodynamics – Shock waves – ISM: clouds – ISM: globules – ISM: kinematics and dynamics

1 INTRODUCTION

Astrophysical media are often strongly clumped, with dense clouds or bullets of cool gas distributed in a far hotter external medium. The flows in these media are complex, particularly when they are perturbed, for example, by outflows from nearby young stars or supernovae.

Insight into these structures be gained by approximate treatments, including multiphase hydrodynamics. Many mass-, momentum- and energy-transfer processes between phases will be important in real flows (Shu et al. 1972; Drew 1983; Kamaya 1997b); similar treatments are used for multiphase space plasma flows, as recently reviewed by Szegö et al. (2000). The simplest cases of pure mass-loading or momentum transfer are interesting limits.

The mass-loading approximation treats the dense cool phase as a distributed source of matter within a hot matrix. It is assumed in this treatment that subsequent to the mass-loading, dissipative processes such as thermal conduction, enhanced by turbulent mixing, mean that the hot phase can be treated as a single, smooth flow. This approximation has been applied, by ourselves and others, to diverse astrophysical objects, such as Wolf-Rayet and planetary nebulae, ultracompact H II regions, starburst galaxies and active galactic nuclei (Chevalier & Clegg 1985; Hartquist et al. 1986; Arthur et al. 1994; Redman et al. 1996; Smith 1996; Williams et al. 1997).

Underlying these approximations are the details of the interaction between a dense clump and a steady wind or a shock have been studied numerically by many authors (e.g. Woodward 1972; Nittman, Falle & Gaskell 1982; Klein, McKee & Colella 1994). Where a strong shock propagates over a dense cloud, these authors find that the cloud is crushed in the direction parallel to the incoming shock, and expands in the lateral direction. Whether the net effect on the cold phase gas can better be described as destruction of the clouds or as a redistribution of their mass spectrum depends on details of radiative and transport processes not included in these simulations.

If the shocks are broadened substantially, the impinging hot material may be treated as a gradually accelerating stream. At least in radiative gas, steady stream interactions may be less destructive than those with rapidly accelerating shocks (Schiano et al. 1995), as a result of sacrificial stripping of small instabilities and of the dissipation of frictional heat input. Indeed, shocks may be able to cause the agglomeration of the condensed material into larger clumps (Kamaya 1997b). The increased pressure of the diffuse gas can also lead to condensation of material into the dense phase, although this depends on details of the thermal evolution.

The results of an interaction with many sources has in general been treated in a continuum approximation: simulations in which the interaction of the flow over numerous obstacles is studied in detail are only just becoming feasible (Jun, Jones & Norman 1996; Poludnenko, Frank & Blackman 2001), and the number of obstacles in these studies is limited. In Fig. 1 of Jun et al., the leading shock is apparently slowed and weakened somewhat by the presence of the clouds, but it is difficult to infer the overall behaviour of the shocks from this paper as only two simulations are illustrated. The finite resolution of such studies leads to numerical viscosity and numerical thermal conduction which can result in far more effective coupling between the phases than might be expected in reality.

In the present paper, we treat the multiphase structure using a momentum-loading formalism. This allows a continuum treatment of the internal structure to maintain the distinction between cool- and hot-phase properties, while including both as dynamically active components of the flow. We parameterize the uncertainty about the detail of the momentum-transfer process by considering separate forms of the coupling terms, and look for general features of the

results. We study the structure of steady shocks in a multiphase ISM in this approximation, for the case in which the two phases ahead of the shock are comoving. This case is somewhat distinct from the formation of termination shocks in an impinging wind driven by mass injection from gas which has been overrun, e.g. in systems such as cometary particle injection in the solar wind (Biermann et al. 1967; Zank & Oughton 1991), or clumps which have been overrun by bubbles driven by stellar winds (Williams et al. 1995) or supernovae (Cowie et al. 1981; Wolff & Durisen 1987; Pittard et al. 2001).

Kamaya has studied the wave dispersion relation (Kamaya 1997a) and time-dependent shock tube problem (Kamaya 1997b) for two phases initially at rest with respect to each other. The time dependent solutions in the latter paper were not integrated for a time sufficient for the two phases to reach equilibrium between the shock and the rarefaction; only one case (with a leading subshock) is presented. Our study complements this work, by determining steady-state structures for a well-defined, if simplified, set of model equations.

We discuss the implications of our results for various astrophysical systems.

2 BASIC EQUATIONS

We consider a system of two phases, a distributed adiabatic hot phase and a clumped cold phase which fills a negligible fraction of the volume of the flow. In reality there will be significant substructure in both the hot and cold phases, but we use continuum equations for both phases on the assumption that a suitable coarse-graining process can provide consistently-defined local mean values for the flow density, velocity and pressure.

We assume that the hot phase obeys mass, momentum and energy equations

$$\frac{\mathrm{d}}{\mathrm{d}x}\left(\rho_1 v_1\right) = 0 \quad (1)$$

$$\frac{\mathrm{d}}{\mathrm{d}x}\left(p+\rho_1 v_1^2\right) = \mathcal{S} \quad (2)$$

$$\frac{\mathrm{d}}{\mathrm{d}x}\left[v_1\left(\frac{\gamma p}{\gamma-1}\right)+\frac{1}{2}\rho_1 v_1^3\right] = \mathcal{S}\left[v_1+\alpha(v_2-v_1)\right], \quad (3)$$

where ρ_1 is the gas density in the hot phase, v_1 is the flow velocity, and p is the pressure. The source term $\mathcal{S}$ is the slip force between the two phases, and α is the fraction of the frictional energy dissipation resulting from this slip which acts to heat the hot phase. In the absence of a second phase ($\mathcal{S}=0$), these equations are simply the equations of steady-state flow for a fluid with adiabatic index γ.

The clumped cold phase obeys the mass and (ballistic) momentum equations

$$\frac{\mathrm{d}}{\mathrm{d}x}\left(\rho_2 v_2\right) = 0 \quad (4)$$

$$\frac{\mathrm{d}}{\mathrm{d}x}\left(\rho_2 v_2^2\right) = -\mathcal{S}, \quad (5)$$

where ρ_2 is the mean density per unit volume of the cold gas, rather than the density within individual clumps. These equations form an autonomous system, as x appears only in the differential operators.

A particularly simple set of equations is used here, considering only momentum-transfer effect. To accurately treat a specific flow, a wide range of mass and energy-transfer processes should also be considered (Shu et al. 1972; Wolff & Durisen 1987). However, the treatment of the astrophysical plasma as consisting of locally uniform interacting media is itself a considerable approximation, and we will see that our further simplification of the system leads to interesting results.

Equations (1), (4) and the sum of equations (2) and (5) can be immediately integrated, to give

$$\Phi_1 = \rho_1 v_1 \quad (6)$$

$$\Phi_2 = \rho_2 v_2 \quad (7)$$

$$p+\rho_1 v_1^2+\rho_2 v_2^2 = \Pi. \quad (8)$$

In addition, $\mathcal{S}$ can be eliminated from equations (1)–(5) to give

$$\frac{\mathrm{d}}{\mathrm{d}x}\left[\frac{\gamma p v_1}{\gamma-1}+\frac{\alpha}{2}\left(\rho_1 v_1^3+\rho_2 v_2^3\right)\right] = (1-\alpha)v_1\frac{\mathrm{d}p}{\mathrm{d}x}. \quad (9)$$

From this equation it is clear that for $\alpha=1$, the total energy flux

$$\mathcal{E} = \frac{\gamma p v_1}{\gamma-1}+\frac{1}{2}(\rho_1 v_1^3+\rho_2 v_2^3) \quad (10)$$

is constant. For $\alpha=0$, the hot flow is adiabatic *so long as there are no discontinuities in the flow*, and hence $p\propto v_1^{-\gamma}$.

For general α, the dependence on x can easily be eliminated, as can those on ρ_1, ρ_2 and p, using the integrals (6)–(8). If the solution is smooth, the result is a first-order o.d.e.

$$\frac{\mathrm{d}v_1}{\mathrm{d}v_2} = \frac{v_1-\alpha(\gamma-1)(v_2-v_1)}{\gamma(\Pi/\Phi_2)-(\gamma+1)(\Phi_1/\Phi_2)v_1-\gamma v_2}. \quad (11)$$

This equation is integrable for all α. However, the cases $\alpha=0$ and $\alpha=1$ are sufficient for our purposes here. We note that this equation depends only on the fraction of the energy deposited in each of the phases, and not on the form of the momentum coupling.

By including the momentum coupling, the full shock structure as a function of x can be derived for each solution of equation (11), using

$$\frac{\mathrm{d}x}{\mathrm{d}v_2} = -\frac{\Phi_2}{\mathcal{S}}. \quad (12)$$

Since $\mathcal{S}$ is a function only of local conditions in the flow, it is clear that v_2 must decrease monotonically through the shock structure (unless $\mathcal{S}=0$ somewhere within the structure).

Dividing equation (11) by equation (12), we find that a critical point exists, as expected, when the flow is at the hot-phase sound speed, i.e., $v_1^2=\gamma p/\rho_1$, or

$$v_1 = \frac{\gamma}{\gamma+1}\frac{\Pi-\Phi_2 v_2}{\Phi_1}. \quad (13)$$

It may be possible for a continuous solution to pass through this critical point if $\mathcal{S}=0$, or if

$$v_2 = \left(1+\frac{1}{\alpha(\gamma-1)}\right)v_1 \quad (14)$$

(for $\alpha\neq 0$).

2.1 Shock solutions

Shock solutions for the basic equations exist where the flow velocity into the discontinuity exceeds the sound speed in the well-coupled limit, i.e.

$$v_{\rm i} > c^\star \equiv \left(\frac{\gamma p_{\rm i}}{\rho_{1,{\rm i}} + \rho_{2,{\rm i}}} \right)^{1/2}, \tag{15}$$

where $\rho_{1,{\rm i}}$ and $\rho_{2,{\rm i}}$ are the upstream densities, $p_{\rm i}$ is the upstream pressure, and $v_{\rm i} = v_{1,{\rm i}} = v_{2,{\rm i}}$ is the upstream velocity.

For $c^\star < v_{\rm i} < c_{1,{\rm i}} \equiv (\gamma p_{\rm i}/\rho_{1,{\rm i}})^{1/2}$, the shock structures will be continuous in both fluids (C-type). For higher velocities the shocks will be led by viscous subshocks in the hot gas (J-type) (following the nomenclature defined for shock waves with magnetic precursors by Draine 1980): as the hot-phase sound speed is the fastest characteristic speed in the undisturbed gas, the subshock must occur at the start of the resolved shock structure. For J-type shocks, the velocity of the hot phase just after the subshock is

$$v_{\rm s} = \frac{\gamma - 1}{\gamma + 1} v_{\rm i} + \frac{2\gamma}{\gamma + 1} \frac{p_{\rm i}}{\Phi_1}, \tag{16}$$

and the pressure is $p_{\rm s} = p_{\rm i} + \Phi_1 (v_{\rm i} - v_{\rm s})$ – the standard Rankine-Hugoniot conditions.

For $\alpha = 1$, energy conservation gives that the final velocity, $v_{\rm f}$, of a shock with upstream velocity $v_{\rm i}$ and pressure $p_{\rm i}$ is given by

$$v_{\rm f} = \frac{\gamma - 1}{\gamma + 1} v_{\rm i} + \frac{2\gamma}{\gamma + 1} \frac{p_{\rm i}}{\Phi_1 + \Phi_2}, \tag{17}$$

whether or not it contains a viscous subshock.

For $\alpha = 0$, the situation is more complex. For C-type shocks, $v_{\rm f}$ is given by

$$p_{\rm i} \left(\frac{v_{\rm i}}{v_{\rm f}} \right)^\gamma + (\Phi_1 + \Phi_2) v_{\rm f} = p_{\rm i} + (\Phi_1 + \Phi_2) v_{\rm i}. \tag{18}$$

For J-type shocks with $v_{\rm i} > c_{1,{\rm i}}$, however, the final velocity, $v_{\rm f}$, is given in terms of $v_{\rm s}$, $p_{\rm s}$ behind the subshock by

$$p_{\rm s} \left(\frac{v_{\rm s}}{v_{\rm f}} \right)^\gamma + (\Phi_1 + \Phi_2) v_{\rm f} = p_{\rm s} + \Phi_1 v_{\rm s} + \Phi_2 v_{\rm i}. \tag{19}$$

The expressions for $v_{\rm f}$ are different for C- and J-type shocks for all $\alpha \neq 1$.

Note that no shock solution can reach a sonic point where equations (13) and (14) are satisfied. We can see this because in order to satisfy these conditions,

$$v_2 = v_2^\star \equiv \left[p_{\rm i} + (\Phi_1 + \Phi_2) v_{\rm i} \right] / \left[\Phi_1 \left(\frac{1+\gamma}{\gamma} \right) \left(\frac{\alpha(\gamma-1)}{1+\alpha(\gamma-1)} \right) + \Phi_2 \right]. \tag{20}$$

If $\gamma > 1$ and $0 < \alpha \leq 1$, $v_2^\star > v_{\rm i}$, but v_2 must decrease monotonically through the shock structure [see the discussion after equation (12) above] so no such critical point can occur in practice.

2.2 Drag force

The spatial structure of the shocks which we calculate is determined by the drag force, $\mathcal{S}$. The simplest assumption is a relation which takes the form of Stokes' law drag (Batchelor 1967), for which

$$\mathcal{S} = \lambda \rho_1 \rho_2 (v_2 - v_1). \tag{21}$$

If the cool phase consisted of isolated, rigid, spherical clouds, then $\lambda = 6\pi R_{\rm c} \nu / M_{\rm c}$, where $R_{\rm c}$ and $M_{\rm c}$ are the radius and mass of the clouds and ν is the kinematic viscosity of the intercloud medium. Interpreted in this direct sense, this law is only valid where the Reynolds numbers $2R_{\rm c}|v_2 - v_1|/\nu 1$, which will not apply in astrophysical situations: at larger Reynolds numbers, the effective drag coefficient increases. While it remains of interest to consider this Stokes' drag force for an arbitrary drag coefficient, the second order term in the expansion for the drag force will cancel the dependence on flow viscosity but introduce a higher order dependence on the slip velocity.

Assuming that the second-order term dominates leads to a drag law proportional to the square of the flow velocity, as used by Shu et al. (1972), a dependence which also corresponds to the 'ballistic' case, where the drag force is calculated by assuming independent collisions of hot-phase particles with the dense clouds. It agrees well with empirical data for rigid projectiles. In the limit which we are considering, of small filling factor of clouds, the drag force may be written

$$\mathcal{S} = C \left(\frac{9\pi\gamma^2}{128} \right)^{1/3} \rho_2 (v_2 - v_1) \frac{\rho_1^{1/3}}{M_{\rm c}^{1/3}} \left(\frac{c_2}{c_1} \right)^{4/3} |v_2 - v_1|, \tag{22}$$

where the typical mass of a cold clump is $M_{\rm c}$ and the typical internal isothermal sound speed is c_2. As above, c_1 is the adiabatic sound speed in the diffuse medium.

An alternative form for the drag force is based on the work of Hartquist et al. (1986, hereafter HDPS), who took into account the effects of deformation of the clouds. These authors considered the dynamics of a flow around a clump in both the subsonic and supersonic limits, assuming that the interaction zones were small enough that each clump interacted with a smooth upstream flow. They determined forms for the mass-loss rate of the clumps, which have been used in subsequent papers to predict a smoothed mass-input rate for the global flow, and agree well with the numerical results of Klein et al. (1994) for strong shocks propagating over isolated clouds. It is a simple matter, however, to reinterpret their results as a momentum transfer: the value is just the mass loss rate between the phases derived by HDPS multiplied by the slip velocity. If the slip speed is slower than the sound speed in the hot phase, we find that the coupling force is given by

$$\mathcal{S} \simeq \rho_2 (v_2 - v_1) \left(\frac{\rho_1 |v_2 - v_1| c_2^2}{M_{\rm c}} \right)^{1/3} \min \left((|v_2 - v_1|/c_1)^{4/3}, 1 \right). \tag{23}$$

We see that in both the Shu et al. and HDPS formulae, the momentum transfer rate is proportional to the mass density in the cool phase divided by the clump mass to the power 1/3: if the cold gas is placed in larger clumps, the ensemble is more permeable to the hot phase flow.

It is of interest to study the results of these forms of slip term in the test-particle limit (i.e. to treat the case in which phase 2 corresponds to a single cloud, and the hot phase velocity is effectively constant). From equations (4) and (5), we find that the velocity of the cloud relative to the hot phase gas is

$$\frac{{\rm d}v_2}{{\rm d}t} = -\frac{\mathcal{S} v_2}{\Phi_2} = -\Lambda v_2^\beta. \tag{24}$$

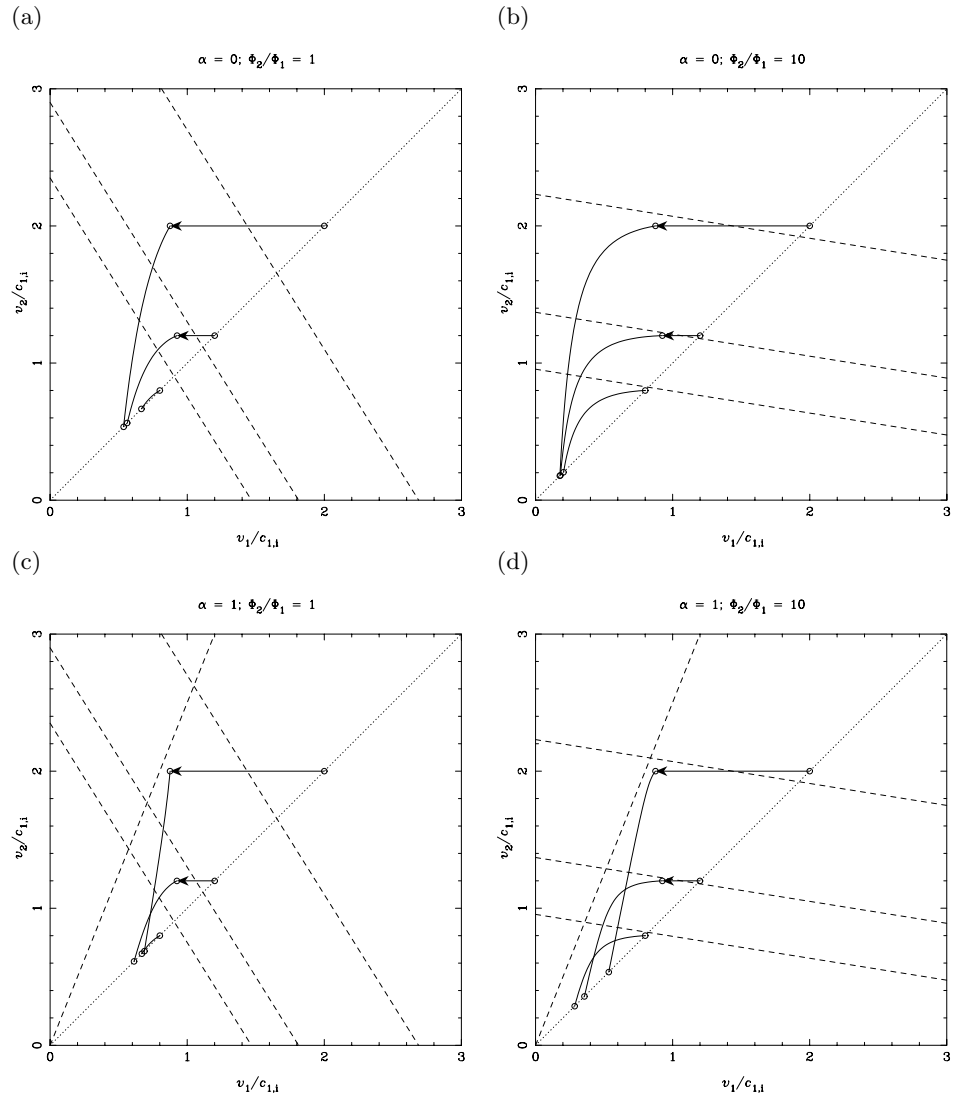

Figure 1. Variation of v_1 and v_2 through resolved shocks for $\alpha = 0$, 1 and density ratios $\Phi_2/\Phi_1 = 1$, 10. Structures for shock Mach numbers $v_{\rm i}/c_{1,{\rm i}} = 2, 1.2, 0.8$ are shown on each plot. Circles show the initial and final states and the solid curve the resolved structure, while the arrow shows the viscous subshock in the structure if one is present. The dotted curve shows the equilibrium condition $v_1 = v_2$, while the dashed lines show the critical conditions $v_1 = c_1$ (for each value of $v_{\rm i}/c_{1,{\rm i}}$) and, for $\alpha = 1$, equation (14).

For Stokes' drag, $\beta = 1$ and $\Lambda = \lambda\rho_1$, while for the (subsonic) HDPS law, $\beta = 8/3$ and Λ is a constant independent of v_2. Integrating, we find that for $\beta = 1$,

$$v_2 = v_{\rm i}\exp(-\Lambda t) \quad (25)$$

$$x = \frac{v_{\rm i}}{\Lambda}\left[1-\exp(-\Lambda t)\right], \quad (26)$$

for $\beta = 2$,

$$v_2 = \frac{v_{\rm i}}{1+\Lambda v_{\rm i} t} \quad (27)$$

$$x = \frac{1}{\Lambda}\log(1+\Lambda v_{\rm i} t), \quad (28)$$

and otherwise

$$v_2 = v_{\rm i}\left[1+(\beta-1)\Lambda v_{\rm i}^{\beta-1}t\right]^{-1/(\beta-1)} \quad (29)$$

$$x = \frac{v_{\rm i}^{2-\beta}}{(\beta-2)\Lambda}\left\{\left[1+(\beta-1)\Lambda v_{\rm i}^{\beta-1}t\right]^{(\beta-2)/(\beta-1)}-1\right\} \quad (30)$$

In the Stokes' drag case, the dense cloud tends to a finite displacement, $v_{\rm i}/\lambda\rho_1$, from its initial position in the diffuse flow. However, for the subsonic HDPS law (and in general for all $\beta \geq 2$) there is no such limit.

This observation relates to d'Alembert's paradox – the prediction of zero drag on a body in irrotational flow, contrasted to practical experience in which turbulence in the wake of bluff bodies maintains drag. For slender bodies in flows of high Reynolds number, very low drag is observed in reality (Batchelor 1967), and so long slip distances could indeed occur for in some cases. We include results for both types of behaviour in what follows.

3 SHOCK STRUCTURES

In Figure 1, we plot the structure of the shocks in drag-coupled two phase media in the (v_1, v_2) plane, for $\alpha = 0$ and

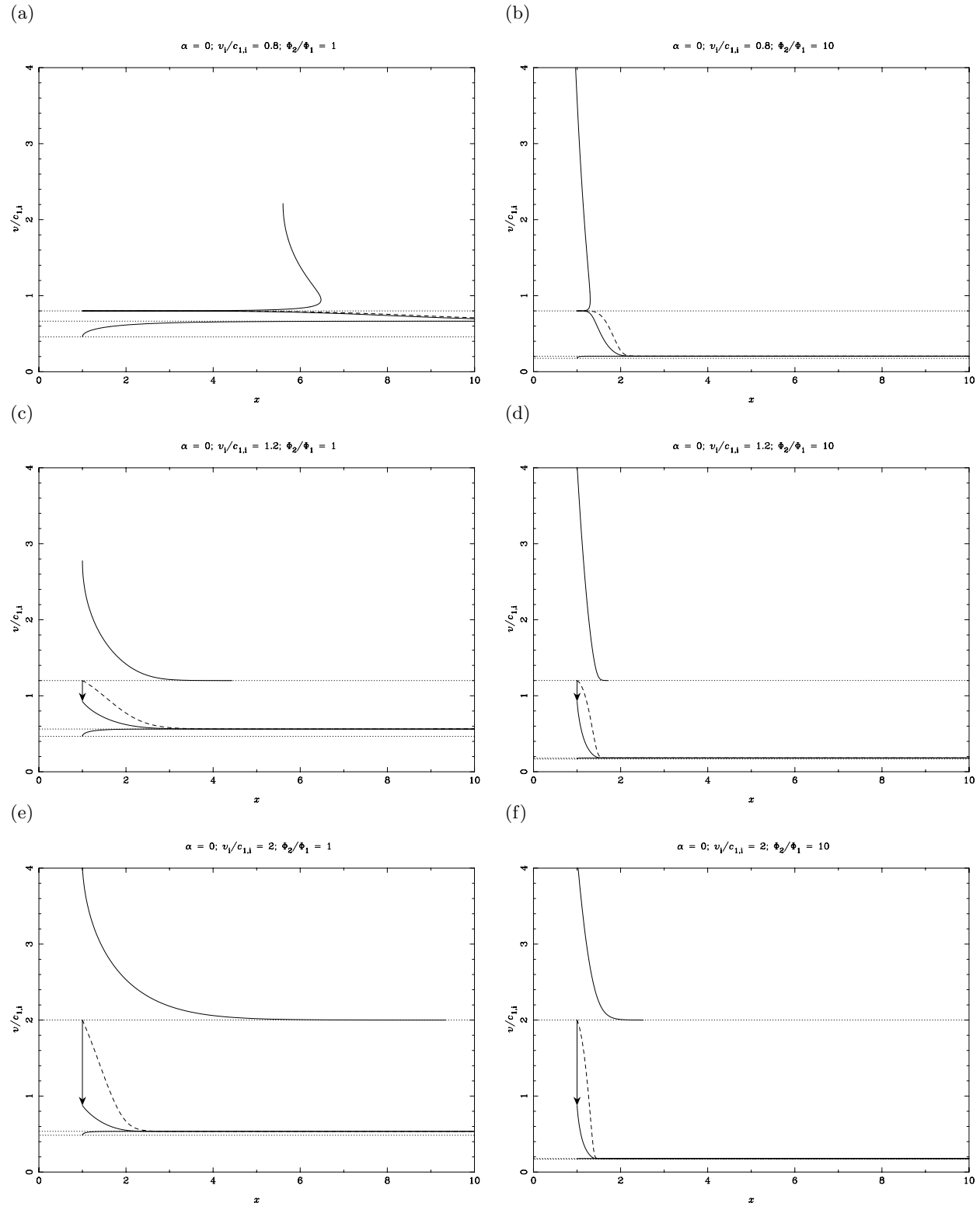

Figure 2. Shock structures for $\alpha = 0$ and various shock Mach numbers $v_{\rm i}/c_{1,{\rm i}}$ and density ratios Φ_2/Φ_1 and with a slip force given by equation (21), for $c_{1,{\rm i}} = \rho_{1,{\rm i}} = 1$. The dotted curves show the initial and final velocities of the shocks, as well as v_1 for a limiting case with $v_2 = 0$ which relaxes to the same final state. The solid curve between the upper dashed lines shows the variation of v_1 through the shock (including the initial subshock for $v_{1,{\rm i}} > c_{1,{\rm i}}$), while the dashed curve shows v_2. Additional solid curves show solutions relaxing to the pre-shock and post-shock equilibrium states.

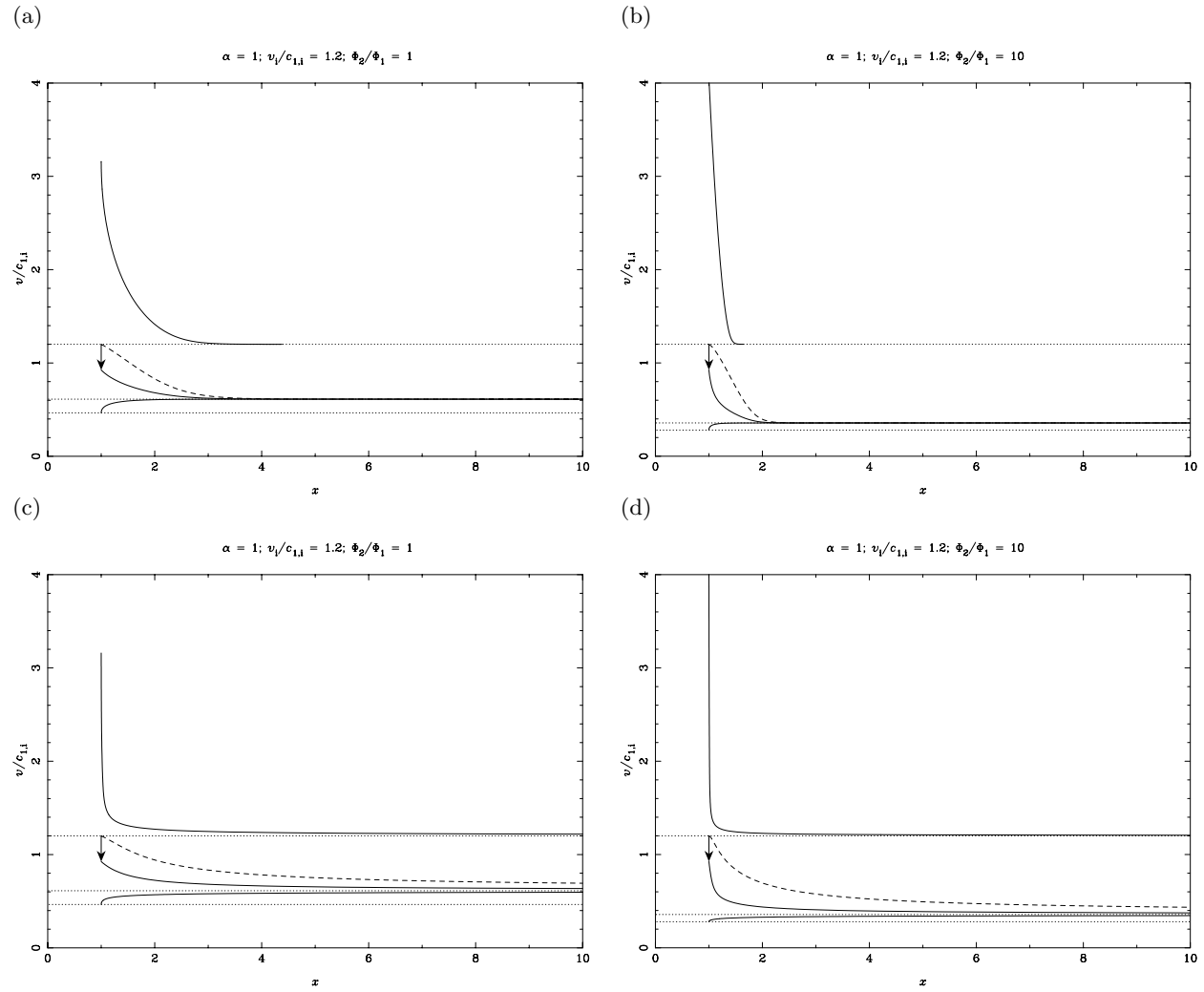

Figure 3. Shock structures for $v_{\rm i}/c_{1,{\rm i}} = 1.2$ as in Figure 2, except that $\alpha = 1$, and for (c), (d) the HDPS slip law is used.

$\alpha = 1$ respectively. These plots are independent of the form of the drag force, $\mathcal{S}$ [cf. equation (11)]. The two columns of these Figures are for a density ratio of $\rho_{1,{\rm i}}/\rho_{2,{\rm i}}$ of $1:1$ and $1:10$, respectively, with curves for several shock Mach numbers (with respect to the adiabatic sound speed in the smooth phase, $c_{1,{\rm i}}$) shown on each plot. For comparison, for a $1:1$ density ratio, the equilibrium critical speed is $c_{1,{\rm i}}/2^{1/2}$, while for a $1:10$ ratio is is $c_{1,{\rm i}}/11^{1/2}$. For $\alpha = 0$, the exhaust velocity of the shocks decreases for the strongest shocks, while for $\alpha = 1$, the exhaust velocity is increased as a result of the energy deposition in the hot phase.

For the weakest shocks, we see that the velocities in the two phases remain very similar, and have continuous (C-type) profiles. For case $\Phi_2/\Phi_1 = 10$, substantial compressions of the medium can be achieved in these C-type shocks. As the shocks strengthen, the smooth phase begins to decrease in velocity significantly before the clumped phase.

Once $v_{\rm i} > c_{1,{\rm i}}$, a viscous subshock is required in the solutions (shown as an arrow), which are hence J-type. It is apparent that, for $\alpha = 0$, increasing clumped-phase density results in a stronger shock (for fixed $v_{\rm i}/c_{1,{\rm i}}$), and more post-shock velocity structure in the smooth phase gas. These effects are less marked for $\alpha = 1$. For shocks with $\alpha = 1$ stronger than those shown here, the smooth-phase gas accelerates after passing through the subshock.

In Figures 2 and 3, we show the internal structure of the shocks as a function of distance, for the Stokes' drag law, equation (21), and for the HDPS slip law, equation (23). The shock structures get narrower as the shock velocity increases, while going from $\alpha = 0$ to $\alpha = 1$ broadens them somewhat. Increased mass flux in the cold phase, Φ_2, appears to narrow the shocks. This is a result of the reduction of the critical speed for the well-coupled limit, which means that for fixed velocity through the upstream gas, the shocks with higher Φ_2 are stronger. Note in particular the extremely small slip velocity between the phases throughout the C-type shock shown in Figure 2(a).

The dashed lines in the Figures show the variation of v_2 through the shock: it is apparent that the velocity difference between the phases increases for stronger shocks. Additional solid lines show supersonic and subsonic equilibria. For shock speeds smaller than the hot-phase sound speed, the solutions of the o.d.e. diverge from the higher-velocity equilibrium solution. As we have previously discussed (Williams & Dyson 1996), the higher-velocity equilibrium solution is not physically unstable, but this solu-

tion topology will occur if fully resolved shock structures are present.

Comparing the results for Stokes' and HDPS drag, we have set the constants of proportionality so the initial post-shock relaxation occurs at a similar rate. It is apparent that the HDPS form leads to an extended post-shock relaxation region, as the small slip velocity in this region leads to decreased effective friction.

3.1 Vorticity

The question of whether the passage of a shock through a clumpy medium smooths out the clumpy structure depends largely on transport processes such as viscosity and thermal conduction (although in astrophysical plasmas, radiative processes can also play an important role). The vorticity produced by the passage of the shock is crucial in enhancing transport processes, as a result of the formation of viscous boundary layers.

If there is a viscous subshock, then the flow is not homoentropic and so Kelvin's circulation theorem (e.g. Batchelor 1967, p273–277) does not hold. Shocks in the flow will generate vorticity when their strength changes across their surfaces. Considering the small scale structures of the flow as the subshock propagates through it, it is apparent that vorticity will be generated in the hot phase where the incident shock refracts around obstacles, and by reflected shocks ahead of them. The forward shock driven into each clump will also lead to creation of vorticity within the clump. This wide distribution of vorticity within the flow will have a significant disruptive effect (cf. Klein, McKee & Colella 1994; Jun, Jones & Norman 1996).

However, if there is no viscous subshock and $\alpha = 0$, the hot-phase flow is homoentropic and (as a result of Kelvin's circulation theorem), the vorticity produced will be entirely confined to the cold phase and the contact between the phases. Even for $\alpha \neq 0$, the generation of vorticity should be confined to the regions of the hot phase flow close to the boundary layers in which the frictional heating is deposited.

As the slip velocity gets smaller, the shear velocities over the surface of individual clumps decrease, and so does the effectiveness with which cool material is entrained from their surfaces. Instead, the cool clumps are rather gently accelerated as they cross the broad shock structure.

We can develop various approximate measures of the destructiveness of the boundary layers induced by passage through a shock. For instance, the amount by which two initially coincident particles, one in each phase, are dragged apart by the front,

$$\Delta x = v_{\rm f} \int_{-\infty}^{\infty} \frac{1}{v_1} - \frac{1}{v_2} dx, \tag{31}$$

where $v_{\rm f}$ is the final equilibrium velocity behind the shock, and v_1 and v_2 are the velocities of the different phases as they pass through it. The value of Δx may be compared to other characteristic lengthscales in the problem. If it is smaller than the size of an individual cold clump, then the passage of the shock will have very little effect on the structure of the medium, while if it is larger than the inter-clump separation, the cool phase will likely be dispersed into a fine aerosol.

Using equation (5) and the Stokes' drag force, equation (21), we find that

$$\Delta x = \frac{v_{\rm f}}{\lambda \rho_{1,i}} \left(1 - \frac{v_{\rm f}}{v_{\rm i}}\right). \tag{32}$$

It is clear that as the shocks weaken or the coupling improves, Δx becomes smaller. By contrast, the slip law of HDPS leads to increasingly poor coupling between the phases at small slip velocities compared to Stokes' drag and the slip distance would be expected to increase for small velocity jumps (cf. Yuan & Wang 1982).

An alternative measure of destructiveness is the maximum slip velocity between the phases. This can be compared, for instance, to the peculiar velocities of the clumps in the upstream multiphase gas: if the maximum slip velocity is smaller than this value, it is difficult to see why the multiphase structure should be substantially effected by the passage of the shock. The interstellar medium has significant structure on large scales, while for a purely hydrodynamic flow in radiative equilibrium, it would be expected that different phases would be dispersed as an aerosol. However, scale lengths are introduced by effects of such as self-gravity (the Jeans length), thermal conduction [the Field (1965) length] or photoionization (the recombination length), resulting in large-scale clumping. If these structures are to form, then they must have a binding energy sufficient to outweigh the higher entropy of the dispersed state.

It is clear, from Figure 1, that the maximum slip velocity decreases rapidly with shock strength. For example, for $\alpha = 0$, the maximum value of the slip velocity, $V = v_2 - v_1$ is given by

$$V^\star = \left(\frac{\Phi_1 + \Phi_2}{\gamma \Phi_2}\right) \left[\left(\frac{v_1^\star}{v_{\rm f}}\right)^\gamma + \gamma \frac{v_{\rm f}^\star}{v_1} - (\gamma + 1)\right] v_1, \tag{33}$$

for a shock with exhaust velocity velocity $v_{\rm f}$, and velocity $v_1^\star$ at the maximum of $V^\star$. As $v_1^\star \to v_{\rm f}$, $V^\star = O[(v_{\rm f} - v_1^\star)^2]$, so for weak shocks the maximum slip velocity decreases rapidly.

If the square of the maximum slip velocity is less than the effective binding energy per unit mass of these structures, then the shock should be able to change the velocity of the flow as a whole without greatly effecting its multiphase structure. While some details of the shock structures vary substantially between different forms of the momentum coupling law, it is in all cases that the maximum slip velocity decreases rapidly as the overall shock velocities decreases below the hot phase critical speed.

4 APPLICATIONS

The relatively benign environment of resolved shocks may have important implications for the evolution of multiphase structures in a wide range of astrophysical circumstances. In the present section, we outline some of those we expect, pending future more detailed investigations.

In Figure 4, we show a schematic picture of the structure of shock-tube problem, in which two gas components collide. The component moving in from the right is smooth, while the component moving in from the left has a clumped structure. If the flows from either side are sufficiently rapid, the solution will take up the usual form of reverse shock, contact discontinuity, forward shock. In Figure 4, we illustrate

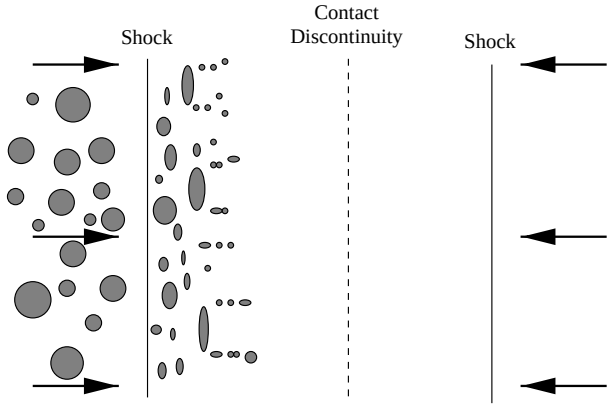

Figure 4. Schematic drawing of the structure of a multiphase shock.

the situation in which the reverse shock into the multiphase medium is of J type: after they pass through the shock, the clumps become elongated and are eventually destroyed (although the deformation of the clumps will obviously be far more complex than that shown in the Figure). If the shock is of C type, however, we have argued that the clumps will be far more gradually decelerated and as a result could remain as fast-moving coherent structures within the protective cocoon of the shocked gas layers.

If a clump slips forwards through the contact discontinuity, its environment will become somewhat more harsh. This will occur if the dense clumps slip through the hot material for a distance larger than that between the shock and the contact discontinuity, or, in an environment which is not plane-parallel, as a result of sideways escape of the diffuse gas. As the forward shock will often be curved, the flow beyond the contact discontinuity will often have significant shear flows. Once a clump passes through the line of the forward shock, however, it will shock directly against the supersonic impinging material and will rapidly dissipate.

This may help explain the survival of knots and bullets in regions such as Orion (Tedds, Brand & Burton 1999) and Eta Carinae (Meaburn et al. 1996). In systems such as these, the spatial density of the bullets may be high enough that they maintain a relatively shared bow-shock, and so reduce the destructive vorticity of the post-shock flow.

It is generally thought that the structures of planetary nebulae are formed when a hot, diffuse wind from a white dwarf remnant overtakes a cool, dense stellar wind blown off during the stars previous evolution along the asymptotic giant branch (Kwok et al. 1978; Mellema 1995). The cool wind is likely to be highly structured, and clumps advected into the hot bubble can have important effects on the global flow (Arthur et al. 1994), as well as being observed in objects such as the Abell 30 (Borkowski et al. 1995). Before they start to interact with the hot stellar wind, these clumps will have had to pass through an outer shock without being destroyed. In particular, the outer region of shocked gas may be broadened substantially, compared to numerical models which have often assumed the cool wind is uniform.

This analysis also provides insight into the structure of the flows around nuclear starbursts (Strickland & Stevens 2000, and references therein). Energy input from supernovae and stellar winds in these starbursts drives plumes of hot gas perpendicular to the plane of the host galaxy, over distances of many kiloparsecs. In the plane of the galaxy, the hot wind from the starburst interacts with the ISM. To date, simulations have in general assumed that the host galaxy ISM may be treated as a smooth gas, at a temperature of $\sim 10^5$ K. This temperature is similar to the mass weighted mean random velocity in the clumpy ISM, and so gives a fairly reasonable impression of the coarse-grained structure of the ISM before the interaction with the nuclear wind begins. Strickland & Stevens (2000) do investigate the effects of mass-loading in some of their models, and find relatively small effects on the flow structure. However, in the galactic plane in their simulations the distributed gas has a temperature of only $\sim 7{\times}10^4$ K, while we find here that the hotter components of the gas will be very important for transmitting pressure waves.

When the nuclear starburst starts to drive a flow outwards in the simulations, the region around the starburst is first evacuated of the ambient ISM gas. After this, a nuclear wind develops which becomes supersonic close to the edge of the starburst mass injection. The resulting nuclear wind shocks against the residual ISM with the usual structure of a forward-shock, a contact discontinuity and a reverse shock. Some cool gas may be dragged away from the galactic plane by shear flows along the contact discontinuity, but in general the structures seen in the galaxy plane are very sharp and well defined.

In contrast, the broadening of the shocks will mean that clouds in the ISM will be rather gradually driven away from the starburst by a diffuse, broad outer shock. The small force on the clouds will result in a secular increase in orbit energy, rather than any dramatic outflow. As a result, in the plane of the galaxy the inner shock and sonic transition around the starburst may take a considerable period to develop. The hot wind from the central nuclear starburst will be surrounded by a weaker wind which has percolated through the ISM, and which carries some shreds of advected cool material along with it.

5 CONCLUSIONS

In this paper, we have discussed the effects which the multiphase nature of a medium can have on the structure of shocks passing through the medium. The shocks rapidly become broader, particularly when the shock speed in the well-coupled limit is smaller than the sound speed in the medium which fills most of the space. We discuss how, in this case, multiphase structure would be expected to survive the passage of the shock.

Broadened multiphase shocks will be important in a wide variety of astrophysical circumstances, as we have discussed above. Equations such as our equations (1)–(5), which model the effects of small-scale structures, can be used in time-dependent hydrodynamical modelling of large-scale structures. For a small computational expense, significant additional insights into the structure of astrophysical flows are available, without the need to resolve the structure of the flow to its finest details.

Acknowledgments

RJRW wishes to thank the PPARC for their support through the award of an Advanced Fellowship, and the Department of Physics and Astronomy, University of Leeds for hospitality while this work was developed.

REFERENCES

Arthur S.J., Dyson J.E., Hartquist T.W., 1994, MNRAS, 269, 1117
Batchelor G.K., 1967, An Introduction to Fluid Mechanics, Cambridge U.P.
Biermann L., Brosowski B., Schmidt H.U., 1967, Solar Physics, 1, 254
Borkowski K.J., Harrington J.P., Tsvetanov Z.I., 1995, ApJ, 449, L143
Chevalier R.A., Clegg A.W., 1985, Nature, 317, 44
Cowie L.L., McKee C.F., Ostriker J.P., 1981, ApJ, 247, 908
Draine B.T., 1980, ApJ, 241, 1021
Drew D.A., 1983, Ann. Rev. Fluid Mech., 15, 261
Field G., 1965, ApJ, 142, 531
Hartquist T.W., Dyson J.E., Pettini M., Smith L.J., 1986, MNRAS, 221, 715 (HDPS)
Jun B.-I., Jones T.W., Norman M.L., 1996, ApJL, 468, 59
Kamaya H., 1997a, ApJ, 474, 308
Kamaya H., 1997b, ApJ, 480, 694
Klein R.I., McKee C.F., Colella P., 1994, ApJ, 420, 213
Kwok S., Purton C.R., Fitzgerald P.M., 1978, ApJ, 219, L125
Meaburn J., Boumis P., Walsh J.R., Steffen W., Holloway A.J., Williams R.J.R., Bryce M., 1996, MNRAS, 282, 1313
Mellema G., 1995, MNRAS, 277, 173
Nittmann J., Falle S.A.E.G., Gaskell P.H., 1982, MNRAS, 201, 833
Pittard J.M., Hartquist T.W., Dyson J.E., 2001, A&A, 373, 1043
Poludnenko A.Y., Frank A., Blackman E.G., 2001, in 'Mass Outflow in Active Galactic Nuclei: New Perspectives', eds. Crenshaw D.M., Kraemer S.B., George I.M., ASP Conf. Ser., in press
Redman M.P., Williams R.J.R., Dyson J.E., 1996, MNRAS, 280, 661
Schiano A.V.R., Christiansen W.A., Knerr J.M., 1995, ApJ, 439, 237
Shu F.H., Milione V., Gebel W., Yuan C., Goldsmith D.W., Roberts W.W., 1972, ApJ, 173, 557
Smith S.J., 1996, ApJ, 473, 773
Strickland D.K., Stevens I.R., 2000, MNRAS, 314, 511
Szegö K., et al., 2000, SSRv, 94, 429
Tedds J.A., Brand P.W.J.L., Burton M.G., 1999, MNRAS, 307, 337
Williams R.J.R., Hartquist T.W., Dyson J.E., 1995, ApJ, 446, 759
Williams R.J.R., Dyson J.E., 1996, MNRAS, 279, 987
Williams R.J.R., Baker A.C., Perry J.J., 1997, MNRAS, 310, 913
Wolff M.T., Durisen R.H., 1987, MNRAS, 224, 701
Woodward P.R., 1972, ApJ, 207, 484
Yuan C., Wang C.Y., 1982, ApJ, 252, 508
Zank G.P., Oughton S., 1991, JGR, 96, 9439